

# Experimental Study of Drift Wave Turbulence in Linear Plasmas\*

Takuma YAMADA, Sanae -I. ITOH, Takashi MARUTA<sup>1)</sup>, Naohiro KASUYA<sup>2)</sup>,  
Shunjiro SHINOHARA<sup>1)</sup>, Yoshihiko NAGASHIMA, Masatoshi YAGI, Kenichiro TERASAKA<sup>1)</sup>,  
Shigeru INAGAKI, Yoshinobu KAWAI, Masayuki FUKAO<sup>3)</sup>, Akihide FUJISAWA<sup>2)</sup>  
and Kimitaka ITOH<sup>2)</sup>

*Research Institute for Applied Mechanics, Kyushu University, Kasuga 816-8580, Japan*

<sup>1)</sup>*Interdisciplinary Graduate School of Engineering Sciences, Kyushu University, Kasuga 816-8580, Japan*

<sup>2)</sup>*National Institute for Fusion Science, Toki 509-5292, Japan*

<sup>3)</sup>*Myojocho, Uji 611-0014, Japan*

(Received 1 December 2007 / Accepted 18 June 2008)

Linear plasmas allow multi-point, low-temperature measurements with Langmuir probes. We measured ion saturation-current fluctuations of a Large Mirror Device-Upgrade linear plasma using a poloidal Langmuir probe array. By varying the discharge conditions, the spatiotemporal behavior showed a change from a coherent sine wave to a turbulent waveform through a periodic, modulated sine wave. The two-dimensional (poloidal wave number and frequency) power spectrum for each regime showed a single fluctuation peak, a peak and its harmonics, and a number of peaks in the poloidal wave number–frequency space. Bi-spectral analysis was performed for the turbulent regime, and showed the existence of nonlinear couplings among fluctuation peaks and broadband components.

© 2008 The Japan Society of Plasma Science and Nuclear Fusion Research

Keywords: linear plasma, drift wave, turbulence, broadband fluctuation, bi-spectral analysis

DOI: 10.1585/pfr.3.044

## 1. Introduction

The study of nonlinear couplings in drift wave turbulence can help our understanding of anomalous transports. Theoretical prediction provides models that indicate that drift waves couple with meso-scale structures, such as zonal flows and streamers [1, 2]. Experimental studies on these nonlinear couplings are in progress, both for linear and toroidal plasmas [3–13]; however, linear plasmas offer the advantage of allowing multi-point, low-temperature measurements with Langmuir probes, and their simple cylindrical shape makes instability models easy to set up. Drift waves are excited by the radial pressure gradient and propagate in the poloidal direction of the plasma cross section. Therefore, multi-point measurements with a poloidal probe array in a linear plasma are useful for understanding drift wave turbulence.

In a Large Mirror Device-Upgrade (LMD-U) linear plasma [14], drift waves and the route to drift wave turbulence were observed [15]. A 64-channel poloidal Langmuir probe array, which can measure the precise poloidal wave numbers of the fluctuations [16], obtained a high-quality, two-dimensional (poloidal wave number  $k_\theta$  and frequency  $\omega$ ) power spectrum of drift wave turbulence. In drift wave turbulence, a number of fluctuation peaks and broadband components appeared in the two-dimensional

power spectrum [17]. In this article, we present a change in the spatiotemporal behavior and two-dimensional power spectrum from a coherent to a turbulent regime. In addition, we identify nonlinear couplings among the fluctuation peaks and broadband components. Bi-spectral analysis, which indicates nonlinear coupling among the three waves, is explained in this section. Section 2 describes the experimental setup, and Secs. 3 and 4 provide results of spectral and bi-spectral analyses, respectively.

Bi-spectral analysis examines the relationship among three waves with frequencies of  $\omega_1, \omega_2$  and  $\omega_3$ , which satisfy the matching condition  $\omega_3 = \omega_1 + \omega_2$ . When the Fourier transformed expression of a temporal waveform  $z(t)$  is  $Z(\omega)$ , the bi-spectrum  $B$  of the three waves is expressed as

$$B = \langle Z(\omega_1)Z(\omega_2)Z^*(\omega_3) \rangle. \quad (1)$$

When the three waves fluctuate independently, the absolute value  $|B|$  becomes 0. When the phases of the three waves are connected by a certain relationship,  $|B|$  becomes finite. The bi-coherence  $b$ , which is a normalized value of  $B$ , and the bi-phase  $\phi_B$ , which indicates the relationship among the phases of the three waves, are expressed as

$$b^2 = \frac{|B|^2}{\langle |Z(\omega_1)Z(\omega_2)|^2 \rangle \langle |Z(\omega_3)|^2 \rangle}, \quad (2)$$

$$\phi_B = \tan^{-1} \frac{\text{Im}(B)}{\text{Re}(B)}. \quad (3)$$

Bi-spectral analysis is important for investigating the cou-

author's e-mail: takuma@riam.kyushu-u.ac.jp

\* This article is based on the invited talk at the 24th JSPF Annual Meeting (2007, Himeji).

pling among three waves. When the bi-coherence  $b$  is finite for the three waves, it suggests that one wave is produced by nonlinear coupling of the other two waves.

## 2. Experimental Setup

The LMD-U linear plasma has a cylindrical shape, with diameter of about 100 mm and axial ( $z$ ) length of 3740 mm. Under the experimental conditions of 3 kW of 7 MHz rf power, 0.01-0.15 T of axial magnetic field (in the  $+z$  direction), and 1-6 mTorr of argon pressure in the source region, the electron density and temperature of the LMD-U plasma are about  $10^{19} \text{ m}^{-3}$  and 3 eV, respectively. The electron density gradient is steep in the radius of  $r = 30\text{-}40$  mm, and produces resistive drift wave instabilities, propagating in the poloidal direction ( $\theta$ ).

The ion saturation-current fluctuations in LMD-U were measured with a 64-channel poloidal Langmuir probe array, shown in Fig. 1. The axial and radial positions of the poloidal probe array are  $z_p = 1885$  and  $r_p = 40$  mm, respectively. Each tungsten probe tip has a diameter of 0.8 mm and is 3 mm long. The 64 probe tips are aligned in the poloidal direction ( $\theta$ ) with 3.9 mm spacing. Mounting the array on a single metal plate aligns the tips precisely, with misalignments of less than 0.1 mm. The probe array measures the poloidal mode number  $m$  of fluctuations up to  $\pm 32$ , where  $m$  is related to the poloidal wave number  $k_\theta$  by  $m = r_p k_\theta$ . The minimum measurable poloidal mode number,  $m = \pm 1$ , corresponds to the poloidal wave number  $k_\theta = \pm 0.025 \text{ mm}^{-1}$ , and the maximum measurable mode number,  $m = \pm 32$ , corresponds to the wave number  $k_\theta = \pm 0.8 \text{ mm}^{-1}$ . The metal plate with the probes is connected to the vacuum flange through a welded bellows. Changing the lengths of the screws around the bellows moves the metal plate in two dimensions in the plasma cross section, and the probe array center can be adjusted to the plasma column center. This is important since  $m = 1$  dominant shift error induces spurious fluctuation modes in

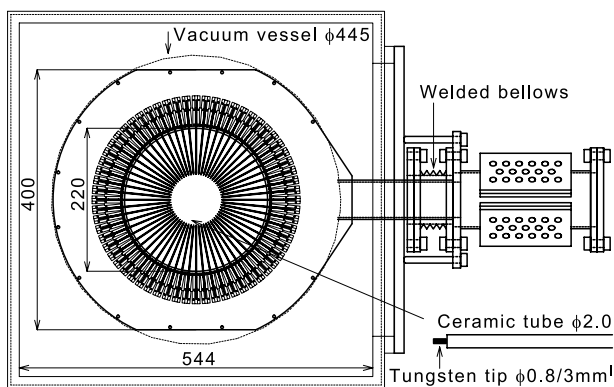


Fig. 1 Schematic view of a 64-channel poloidal Langmuir probe array. The measuring radius is 40 mm. The probe array is connected to a vacuum flange through a welded bellows so that it moves in two dimensions.

the poloidal mode number space by coupling with the real fluctuation modes [16].

Increasing the magnetic field or decreasing the argon pressure changes the regime from coherent to turbulent. Figure 2 shows the spatiotemporal fluctuations of the ion saturation-current measured with the 64-channel probe array. The discharge conditions of the magnetic field and argon pressure are (a) 0.02 T and 2 mTorr, (b) 0.09 T and 6 mTorr, and (c) 0.09 T and 2 mTorr, respectively. The increasing direction of the poloidal angle  $\theta$  corresponds to the electron diamagnetic direction. The waveform of (a) is a coherent sine wave with poloidal mode number  $m = 3$ .

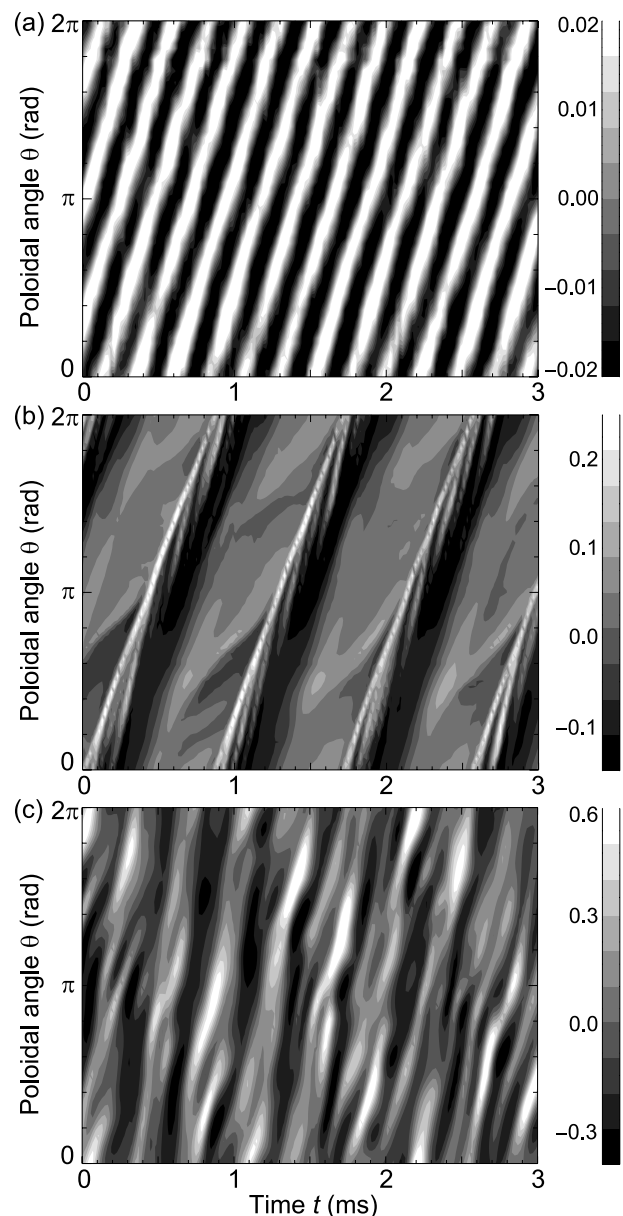


Fig. 2 Spatiotemporal behavior of ion saturation-current fluctuations (arb. unit) measured with the 64-channel poloidal probe array. The discharge conditions (magnetic field and argon pressure) are (a) (0.02 T, 2 mTorr), (b) (0.09 T, 6 mTorr), and (c) (0.09 T, 2 mTorr).

Only a single instability mode of  $m = 3$  in the electron diamagnetic direction is excited in the plasma. The straight lines in the figure show that the probe array measurements are performed with a good symmetry in the plasma cross section, due to the fine positioning of the probe array. The waveform of (b) is a periodic waveform with  $m = 1$ . Periodic positive spikes and some modulations with  $m \geq 2$  are seen. The waveform of (c) shows that the plasma is in a turbulent regime and is not a periodic waveform. There is a main  $m = 1$  fluctuation in the electron diamagnetic direction, together with complex structures separating and combining.

In conclusion, varying the discharge conditions changes the plasma from (a) a coherent regime to (b) a periodic regime, to (c) a turbulent regime. Further analysis is performed by two-dimensional spectral analysis.

### 3. Spectral Analysis

The power spectrum of the ion saturation-current fluctuation in each regime, explained in the previous section, was calculated by two-dimensional Fourier transformation (from poloidal angle  $\theta$  to poloidal mode number  $m$ , and from time  $t$  to frequency  $f = \omega/2\pi$ ). Figure 3 shows the two-dimensional power spectra  $S(m, f)$  of Figs. 2(a)-(c). An average of the results from 300 time windows (each time window is 10 ms long) during discharges was used to derive each power spectrum  $S(m, f)$ . A two-dimensional Fourier transformation can determine the poloidal propagating directions of the fluctuations by the signs of the poloidal mode number  $m$  (when the frequency is set to  $f \geq 0$ ). Positive and negative mode numbers correspond to the electron and ion diamagnetic directions, respectively. This feature is a great advantage over single-probe measurements.

The power spectrum in the coherent regime (Fig. 3(a)) shows only a single fluctuation peak at  $(m, f) = (3, 4.2 \text{ kHz})$ ; therefore, a coherent sine wave is observed in the spatiotemporal behavior. The density fluctuation (the ion saturation-current fluctuation) leads the potential fluctuation (the floating potential fluctuation) by 10-30 degrees, and the normalized density fluctuation level is comparable to the normalized potential fluctuation level. This indicates that the observed instability mode was a drift wave mode [15]. Drift wave instabilities with  $m \neq 3$  were damped and only the  $m = 3$  mode remained.

The power spectrum in the periodic regime (Fig. 3(b)) shows some fluctuation peaks with the relationship of  $f [\text{kHz}] = 1.15 m$ , which is shown by a dashed line. The peak at  $(m, f) = (1, 1.15 \text{ kHz})$  is considered the standard drift wave mode excited in the plasma, and the others are harmonics of the standard wave. Up to the eighth harmonic are seen in the figure. The harmonics are excited by self-nonlinear couplings of the standard mode. Therefore, the spatiotemporal behavior shows a quasi-periodic structure with a modulated sine wave. These harmonics

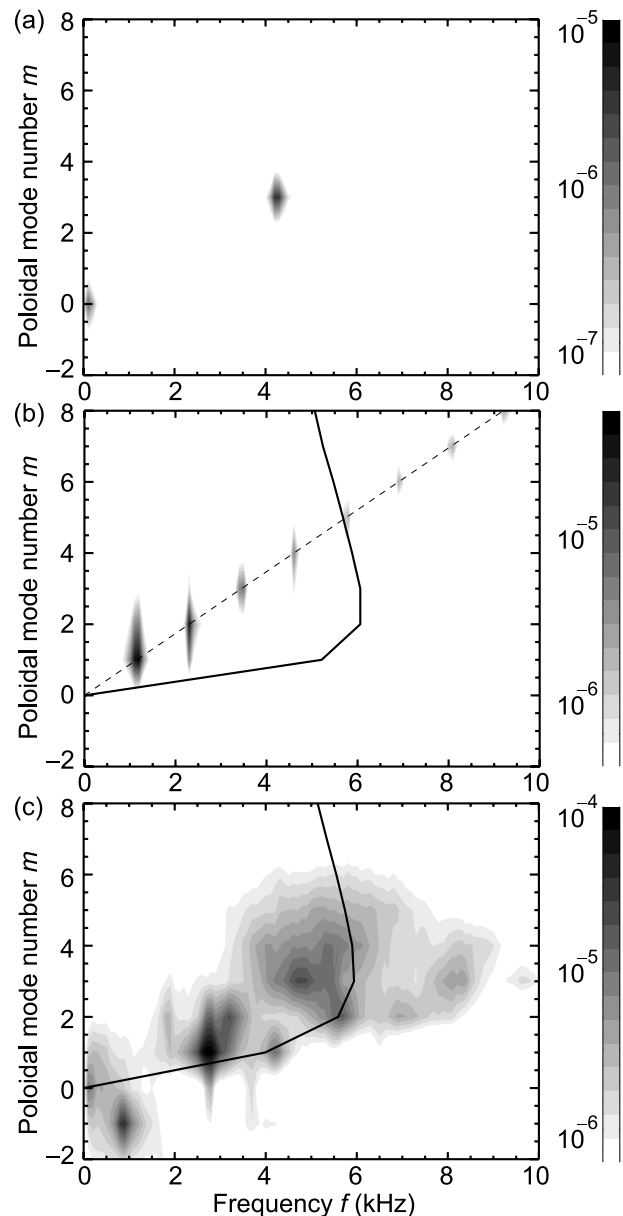


Fig. 3 Contour plots of two-dimensional power spectra  $S(m, f)$  (arb. unit) for each discharge shown in Figs. 2(a)-(c). The dashed line in (b) shows the relationship  $f [\text{kHz}] = 1.15 m$ . The solid lines in (b) and (c) show linear dispersion relations of drift waves, calculated by numerical code analyses.

are non-mode peaks, since drift waves in plasmas do not show straight linear dispersion relationships in  $m$ - $f$  space, and the harmonics do not satisfy the linear dispersion relationship. The solid line in the figure indicates the linear dispersion relationship of drift waves calculated by numerical code analysis [18]. The line shows the case with no dc radial electric field. In reality, there is a dc radial electric field inside the plasma, which rotates the plasma by  $\mathbf{E} \times \mathbf{B}$  drift with a frequency of  $f_{E \times B}$ ; it is not currently accurately measurable at LMD-U. The linear dispersion relation is modified by  $f_{E \times B}$  by subtracting  $m \cdot f_{E \times B}$  from the eigen-

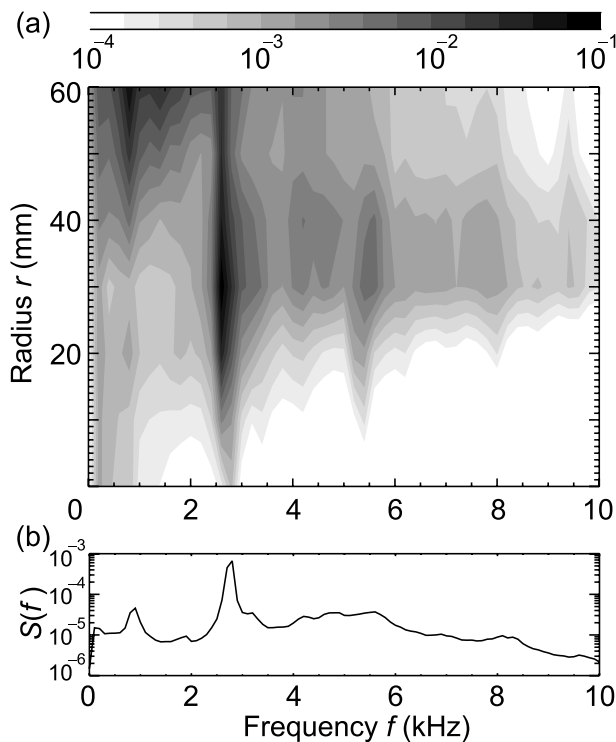


Fig. 4 (a) The radial profile of power spectrum (arb. unit) of relative ion saturation-current fluctuation in a turbulence regime. A radially movable Langmuir probe was used. The discharge conditions (magnetic field and argon pressure) are (0.02 T, 2 mTorr). (b) The power spectrum (arb. unit) at  $r = 40$  mm.

frequencies. The radial electric field is of the order of O (10 V/m), so that  $f_{E \times B}$  is of the order of O [kHz]. Therefore, the standard mode can be understood as a drift wave mode.

The power spectrum in the turbulent regime (Fig. 3(c)) shows a number of fluctuation peaks in  $m$ - $f$  space. Figure 4 shows the results of the same discharge conditions measured with a single probe. Figure 4(a) shows the radial profile of the power spectrum  $S(r, f)$  measured with a radially movable probe [15], and Fig. 4(b) shows the power spectrum  $S(f)$  at  $r = 40$  mm measured with one probe of the 64-channel probe array. The two-dimensional power spectrum  $S(m, f)$  contains more information than the power spectrum  $S(f)$  measured with a single probe. The broadband spectrum seen in Fig. 4(b) reveals some fluctuation peaks in  $m$ - $f$  space by decomposing into poloidal mode numbers.

The fluctuation peaks in Fig. 3(c) do not satisfy a single proportional relationship between  $m$  and  $f$ . Therefore, more than one unstable mode is excited in the plasma. Some of the peaks are excited by nonlinear couplings between other peaks. The strongest peak in  $m$ - $f$  space is at  $(m, f) = (1, 2.8 \text{ kHz})$ . This fluctuation peak has a strong intensity at a steep gradient region in the plasma electron density profile (see Fig. 4(a)), and is considered a

drift wave mode [15]. The peaks at  $(m, f) = (2, 5.6 \text{ kHz})$  and  $(3, 8.4 \text{ kHz})$  must be harmonics of the peak  $(m, f) = (1, 2.8 \text{ kHz})$  produced by self-nonlinear couplings, since these satisfy the relationship of  $f$  [kHz] = 2.8  $m$ . Other peaks are excited instability modes or peaks excited by nonlinear couplings. For instance, the fluctuation peak at  $(m, f) = (-1, 0.9 \text{ kHz})$  in the ion diamagnetic direction is not a drift wave mode, since its intensity is strong in the plasma edge region, rather than the steep gradient region (see Fig. 4(a)). The solid line in the figure again shows the calculated linear dispersion relation of drift waves with no dc radial electric field. Several unstable modes, including  $(m, f) = (1, 2.8 \text{ kHz})$  in the  $m$ - $f$  plane (except  $(m, f) = (-1, 0.9 \text{ kHz})$ ), must satisfy the dispersion relation by considering the dc electric field.

In addition, there are broadband fluctuation components other than the fluctuation peaks. These are also considered to be produced by nonlinear couplings. Identification of the nonlinear couplings by bi-spectral analysis is discussed in the next section.

#### 4. Bi-Spectral Analysis

Nonlinear couplings in the turbulent regime are confirmed by bi-spectral analysis, as shown below. Whether three waves with frequencies of  $f_1$ ,  $f_2$ , and  $f_1 + f_2$  fluctuate independently or dependently is judged by bi-spectral analysis. Bi-spectral analysis was applied to prove the nonlinear couplings among the fluctuation peaks that appear in Fig. 3(c). Figure 5 shows the squared bi-coherence of the ion saturation-current fluctuation measured with a single probe. The frequency range is 0-10 kHz. The result was an ensemble of 300 time windows (each time window is 10 ms long). The white region indicates that the three waves have no relationships, and the dark region indicates that a phase relationship exists among the three waves; therefore, one wave is excited by nonlinear coupling of the rest of the waves.

The dark lines,  $f_{1,2} = 0.9$  and 2.8 kHz, indicate that the fluctuation peaks  $(m, f) = (1, 2.8 \text{ kHz})$  and  $(-1, 0.9 \text{ kHz})$  in Fig. 3(c) couple with many other fluctuation peaks and also with broadband components. Self-nonlinear coupling of  $(m, f) = (1, 2.8 \text{ kHz})$  is weak, but above the confidence level of 0.003 ( $= 1/300$ ). Coupling between  $(m, f) = (1, 2.8 \text{ kHz})$  and  $(2, 5.6 \text{ kHz})$  to produce the third harmonic is significantly strong. Other strong and weak couplings are seen everywhere in  $f_1$ - $f_2$  space. For instance, the non-drift wave mode  $(m, f) = (-1, 0.9 \text{ kHz})$  couples strongly with the frequency of 4.7 kHz, whose poloidal mode number is estimated to be three by Fig. 3(c). This coupling indicates the three wave couplings in Fig. 3(c) of  $(m, f) = (-1, 0.9 \text{ kHz}) + (3, 4.7 \text{ kHz}) = (2, 5.6 \text{ kHz})$ , which are expected from previous work [15]. (An exhaustive analysis of peak decomposition, shown in Fig. 5, will be discussed in a future report.) The weak and broad couplings in the  $f_{1,2} > 4 \text{ kHz}$  region indicate couplings among

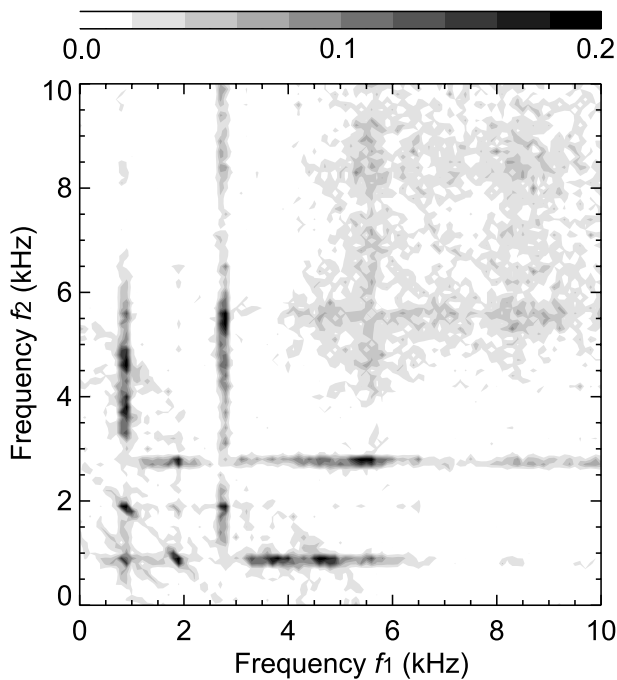


Fig. 5 Squared bi-coherence of ion saturation-current fluctuation in  $f$ - $f$  space. The discharge conditions are same as those for Fig. 4. The confidence level is 0.003. Dark regions indicate nonlinear couplings among three fluctuations with frequencies  $f_1$ ,  $f_2$ , and  $f_1 + f_2$ .

broadband components. Thus, non-mode excitations from a few excited modes were confirmed by bi-spectral analysis. Drift wave turbulence is produced by nonlinear couplings among a few parent modes.

## 5. Summary

We measured the spatiotemporal behavior and two-dimensional power spectra of the ion saturation-current fluctuations in an LMD-U linear plasma using a 64-channel poloidal probe array. By varying the discharge conditions, i.e., the magnetic field and argon pressure, the behavior changed from a coherent to a turbulent regime, passing through a periodic regime. The coherent regime showed a single fluctuation peak in  $m$ - $f$  space. The periodic regime showed a standard fluctuation peak and its harmonics. The turbulent regime showed a number of

fluctuation peaks with more than one primary mode. The nonlinear couplings among the fluctuation peaks and broadband components in the turbulent regime were confirmed by bi-spectral analysis.

Bi-spectral analysis can be extended to two dimensions by considering the matching condition of the poloidal wave number. The 64-channel poloidal probe array is able to measure the precise poloidal wave number. Therefore, two-dimensional bi-spectral analysis in  $k_\theta$ - $\omega$  space is planned for future work.

## Acknowledgments

This work was supported by a Grant-in-Aid for Specially-Promoted Research of MEXT (16002005) (Itoh Project), by Grant-in-Aid for Young Scientists (B) of JSPS (19760597), and by the collaboration programs of NIFS (NIFS07KOAP017) and RIAM, Kyushu University.

- [1] P.H. Diamond *et al.*, Plasma Phys. Control. Fusion **47**, R35 (2005).
- [2] A. Yoshizawa, S.-I. Itoh and K. Itoh, *Plasma and Fluid Turbulence, Theory and Modelling* (Institute of Physics Publishing, Bristol and Philadelphia, 2003).
- [3] T. Klinger *et al.*, Phys. Rev. Lett. **79**, 3913 (1997).
- [4] M. Kono and M.Y. Tanaka, Phys. Rev. Lett. **84**, 4369 (2000).
- [5] C. Schröder *et al.*, Phys. Rev. Lett. **86**, 5711 (2001).
- [6] T. Kaneko, H. Tsunoyama and R. Hatakeyama, Phys. Rev. Lett. **90**, 125001 (2003).
- [7] V. Sokolov and A.K. Sen, Phys. Rev. Lett. **92**, 165002 (2004).
- [8] M.J. Burin *et al.*, Phys. Plasmas **12**, 052320 (2005).
- [9] G.R. Tynan *et al.*, Plasma Phys. Control. Fusion **48**, S51 (2006).
- [10] C. Lechte, S. Niedner and U. Stroth, New J. Phys. **4**, 34 (2002).
- [11] Y. Nagashima *et al.*, Phys. Rev. Lett. **95**, 095002 (2005).
- [12] Y. Hamada *et al.*, Phys. Rev. Lett. **96**, 115003 (2006).
- [13] F.M. Poli *et al.*, Phys. Plasmas **13**, 102104 (2006).
- [14] S. Shinohara *et al.*, *Proc. 28th Int. Conf. on Phenomena in Ionized Gases* (Institute of Plasma Physics AS CR, Prague, 2007), 1P04-08.
- [15] K. Terasaka *et al.*, Plasma Fusion Res. **2**, 031 (2007).
- [16] T. Yamada *et al.*, Rev. Sci. Instrum. **78**, 123501 (2007).
- [17] T. Yamada *et al.*, Plasma Fusion Res. **2**, 051 (2007).
- [18] N. Kasuya *et al.*, J. Phys. Soc. Jpn. **76**, 044501 (2007).